High-Pressure Speed of Sound Measurements of trans-1-Chloro-3,3,3-trifluoropropene (R1233zd(E)) in Liquid Region for Temperature from (273.15 to 353.15) K

High pressure speed of sound measurements of trans-1-chloro-3,3,3-trifluoropropene (R1233zd(E)) in the subcooled liquid region for temperature from (273.15 to 353.15) K

S. Lago,*,† P. A. Giuliano Albo,† J. S. Brown,‡ and M. Bertinetti†

†*Istituto Nazionale di Ricerca Metrologica*

‡*Catholic University of America*

E-mail: s.lago@inrim.it

Abstract

This paper presents subcooled liquid speed of sound measurements of trans-1-chloro-3,3,3-trifluoropropene (CAS Number 102687-65-0; R1233zd(E)) along six isotherms over the temperature range from (273.15 to 353.15) K for pressures up to 35 MPa by means of the double pulse-echo method. The expanded uncertainty at a confidence level of 95 % of the speed of sound measurements is 0.08 %. The experimental results were compared with predictions from the state-of-the-art Fundamental Helmholtz Energy equation of state[1].

Key words: high pressure, R1233zd(E), speed of sound, trans-1-chloro-3,3,3-trifluoroprop-1-ene

Introduction

Trans-1-chloro-3,3,3-trifluoroprop-1-ene (R1233zd(E)) is a refrigerant characterized by a somewhat low vapor pressure that is approximately 10 % to 20 % lower than the one of 1,1,1,3,3-penafluoropropane (R245fa) depending on the temperature. More interesting, the vapor pressure of R1233zd(E) is about 30 %, and up to 50 %, higher than the one of 2,2-dichloro-1,1,1-trifluoroethane (R123) that, together with R245fa, is widely used in centrifugal chiller applications.

R1233zd(E) is non-toxic and non-flammable and is thus classified by ASHRAE as a Class A1 refrigerant.[2] It possesses attractive environmental characteristics with an estimated ozone depletion potential of 0.0005 and an estimated global warming potential of less than 14.[3] Given its combination of thermodynamic properties, safety profile, and environmental characteristics, it is considered to be an interesting alternative working fluid for chiller applications, high-temperature heat pumps, and organic Rankine cycles.[3]

The publicly available literature contains three datasets of saturated vapor pressure[1,4,5], four datasets of compressed liquid density,[1,4–6], three datasets of vapor phase pvT[1,4,7], one dataset of saturated liquid density,[5] one dataset of compressed liquid speed of sound measurements,[1] one dataset of surface tension measurements,[8] and a fundamental Helmholtz equation of state,[1] which has been implemented in.[9]

The present authors wish to contribute to the database of available property measurements for R1233zd(E) by reporting speed of sound measurements in the subcooled liquid phase over the temperature range from (273.15 to 353.15) K.

Experimental measurements

The test sample of trans-1-chloro-3,3,3-trifluoropropene (CAS Number 102687-65-0) was supplied by Central Glass Co., Ltd. with a declared purity greater than 0.995 in mass fraction. While there was no attempt to further purify the sample by the authors, the declared purity is more than sufficient for the present purposes since the effects of impurities at these levels on liquid speed of sound measurements are negligible, particularly

when compared to the other sources of uncertainty.

Speed of sound measurements technique and apparatus

In the present work, a transient technique[10] was utilized for the speed of sound measurements. The technique involves determining the speed of sound from two mechanical quantities: the length of the acoustic paths traveled by two separate ultrasonic tone bursts and the associated time intervals, in particular the experimental apparatus has been designed on the double pulse-echo method. In the present implementation, an electric tone-burst is used to excite the piezoelectric source by an acoustic wave packet (five cycles with a carrier frequency of about 4 MHz and an amplitude of 10 V_{pp}), an ultrasonic signal spreads in opposite directions into the test sample (maintained at a specified thermodynamic equilibrium state determined by its temperature and pressure), hitting two reflectors placed at unequal distances from the source. Then by measuring the time of flight of the waves and by knowing the acoustic path length, the speed of sound can be determined.

Speed of sound measurements can be considered absolute when they are obtained from direct measurements of length and time, and are considered to be relative when they are measured with respect to the speed of sound of a known and well-characterized reference fluid.

Transient techniques assume that emitted ultrasonic burst spreads as a plane-waves thus with plane-fronts and with the acoustic pressure having the same phase of the particles speed. For any kind of source, this approximation usually holds when the tone burst has travelled a minimum distance from the source. This effect is, mainly, due to the limited dimension of the source and the wave-like nature of the emitted tone burst. The physical description is particularly difficult since it is a problem of wave radiation and available analytic solutions are limited to few cases that usually include approximations. However, whatever is the description and the adopted approximations, all the results agree on the existence of a separation between the space closed to the source (*near-field*) and that one far away (*far-field*)[11] and the plane-wave approximation holds only in the

far-field of the source. In the case of disc sources, the calculated limit varies as a function of the source diameter, the carrier frequency and the speed of sound, thus the limit moves when measurements are carried out in wide ranges of temperature and pressure. Despite an accurate evaluation of the needed minimum distance is difficult to be calculated, it has been chosen to use the approximation considering that the source disc emits continuous waves at a frequency of 4 MHz, that is the same frequency used as carrier of the tone burst.

Since for the subcooled liquid measurements presented herein the speed of sound values are relatively low, it was critically important to carefully design the lengths of the spacers by taking into account the diameter of the source and the working frequency. With this goal in mind, the apparatus was tested using various carrier frequencies to check the repeatability of the measured values and to evaluate *near-field* effects (observed if the time-of-flight values differ more by more than 20 ppm at different frequencies). If for a given carrier frequency *near-field* effects were observed, then the carrier frequency was reduced until agreement was finally reached for the time-of-flight values.[12]

If a source transducer does not have the necessary band-width to work at different frequencies, it is necessary to design cells with increased spacer lengths. In order to verify repeatability of the speed of sound measurements, two different sensors (with AISI-316L stainless steel spacers) were tested. The first test cell (Figure 1a) had spacers with nominal lengths of (30 and 45) mm and the second test cell (Figure 1b) had spacers with the nominal lengths of (67 and 45) mm. These two sensors were chosen because they possess path lengths that provide an acceptable trade-off between shorter distances (better signal to noise ratio although approaching the near-field of the source) and longer distances (increased accuracy although lower signal-to-noise ratio.)

The difference in the acoustic path lengths of the cell was determined at ambient conditions ($T = 293.99$ K and $p = 0.097$ MPa) by comparing measurements of degassed Millipore ultra-quality water to calculated speed of sound values as determined by the 1995 equation-of-state of the International Association for the Properties of Water and Steam (IAPWS-95) which, for the above described state point, has an uncertainty of

0.005 %,[13] according to the procedure described in[14] and.[15]

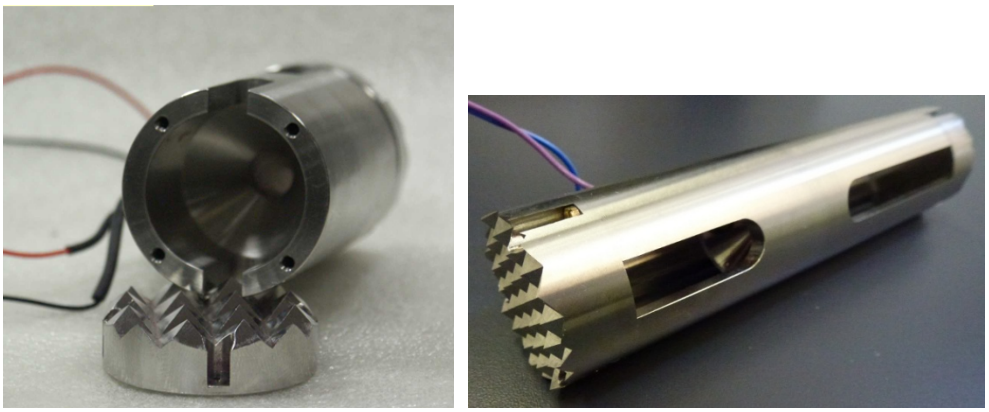

(a) (b)

Figure 1: (a) Test Cell 1 with nominal spacers dimensions of (30 and 45) mm. Figure 1b(b) Test Cell 2 with nominal spacers dimensions of (45 and 67) mm.

While making measurements, the ultrasonic test cell was placed inside an evacuated and pressure-tight stainless steel chamber. Pressure was imposed and maintained by a pressure amplifier connected to the sample canister. The pressure was measured with a transducer possessing a maximum uncertainty of 0.05 MPa. The transducer's hysteresis effects, ion the order of 0.025 MPa, are within the overall uncertainty of the transducer.

The desired sample temperature was established and uniformly maintained by immersing the high pressure test vessel in a continuously stirred thermostatic bath regulated by a PolyScience thermostat with a stability of 0.01 K, and a second stage internal PID controller operating with a platinum resistance probe and two 250 W heaters (normally operating at a maximum power of 4 W). The thermostat was able to achieve temperature stability of $\pm$ 1 mK over the entire operating temperature range. The temperature associated with the speed of sound measurements was determined, as the average of two platinum resistance thermometers (PRTs) (located on the top and the bottom of the pressure vessel) and calibrated against a standard PRT. The temperature gradient of the PRTs was within 10 mK.[16] contains a detailed description of the complete apparatus and of the experimental technique.

Experimental speed of sound measurement procedure and results comparison.

For each isotherm, fresh sample was loaded into the high pressure vessel by means of a manual piston-type pump up to selected pressure.

The measurements were taken along six isotherms for temperatures ranging from (273.15 to 353.15) K, beginning at the highest pressure level (35 MPa) and proceeding by decrementing the pressure in steps until nearly reaching atmospheric pressure (or a pressure with an acceptable signal-to-noise ratio which depended on the temperature.) The pressure decrements occurred in steps of 5 MPa near the upper boundary, steps of 10 MPa in the middle of the isotherm, and steps of less than 4 MPa near the minimum pressure values, resulting in nominal pressure values of (35, 30, 25, 20, 10, 5, 1, and 0.3) MPa. The system was evacuated before making measurements along an isotherm in order to ensure a complete refill with fresh sample.

Since changing the sample pressure resulted in a corresponding temperature change, it was necessary to wait approximately 1.5 hours for thermal equilibrium, at the desired temperature, to be re-established so that a new speed of sound measurement could be taken for the newly established pressure value.

The experimental results were fitted to a bi-dimensional polynomial surface and the realigned values were calculated to agree with the nominal thermodynamic state points. The degree of the bi-dimensional polynomial was chosen so that the differences between the experimental values and the ones calculated from the polynomial itself were less than 10 % of the expanded speed of sound uncertainty.

Table 1 provides the speed of sound data on the regular mesh obtained by the following bi-dimensional polynomial equation:

$$w\left(T,p\right)=\sum_{i=0}^{2}\sum_{j=0}^{4}a_{ij}\left(T-T_{0}\right)^{i}\left(p-p_{0}\right)^{j} \tag{1}$$

where the a_{ij} coefficients are provided in Table 2.

The speed of sound data also are provided in Figure 2 and Figure 3 as functions of

temperature and pressure, respectively.

Table 1: **Speed of sound measurements of subcooled liquid R1233zd(E).**

p/MPa	w/m s^{-1}	p/MPa	w/m s^{-1}	p/MPa	w/m s^{-1}	p/MPa	w/m s^{-1}	p/MPa	w/m s^{-1}
				273.15 K					
0.3	787.503	1.0	791.741	2.0	797.718	5.0	815.122	10.0	842.505
20.0	892.134	25.0	914.855	30.0	936.462	35.0	957.137		
				293.15 K					
0.3	707.917	1.0	712.894	2.0	719.877	5.0	739.987	10.0	771.062
20.0	826.217	25.0	851.174	30.0	874.737	35.0	896.992		
				313.15 K					
0.3	628.747	1.0	634.662	2.0	642.917	5.0	666.411	10.0	701.973
20.0	763.439	25.0	790.817	30.0	816.472	35.0	840.436		
				333.15 K					
0.3	549.992	1.0	557.044	2.0	566.837	5.0	594.393	10.0	635.237
20.0	703.799	25.0	733.782	30.0	761.666	35.0	787.469		
				353.15 K					
0.3	471.651	1.0	480.041	2.0	491.639	5.0	523.934	10.0	570.856
20.0	647.297	25.0	680.069	30.0	710.321	35.0	738.091		

Table 2: **Coefficients of Eq. 1 calculated for $T_0 = 313$ K and $p_0 = 15$ MPa.**

$a_{00} = 734.500$	$a_{01} = 6.1171$	$a_{02} = -5.21039 \cdot 10^{-2}$	$a_{03} = 9.79486 \cdot 10^{-4}$	$a_{04} = -1.87059 \cdot 10^{-5}$
$a_{10} = -3.2106$	$a_{11} = 3.29086 \cdot 10^{-2}$	$a_{12} = -7.25345 \cdot 10^{-4}$	$a_{13} = 2.30982 \cdot 10^{-5}$	$a_{14} = -5.10209 \cdot 10^{-7}$
$a_{20} = 3.55510 \cdot 10^{-3}$	$a_{21} = 9.39874 \cdot 10^{-5}$	$a_{22} = -4.84760 \cdot 10^{-6}$	$a_{23} = 1.62674 \cdot 10^{-7}$	$a_{24} = -1.94390 \cdot 10^{-9}$

The first measurements were taken for the isotherm of 293 K, followed by the isotherms of 313 K, 333 K, and 353 K. However, for the measurements at 353 K and at 25 MPa, polymerization was observed. At this point, the piezoelectric transducer was changed in order to ensure purity of the test samples. Moreover, in order to obtain measurements in a second and independent way, the ultrasonic sensor was changed as well.

However, before making measurements for the two missing isotherms (283 K and 272 K), measurements were repeated for the isotherm of 293 K in order to verify the consistency of the results obtained from the two different measuring cells. In addition, some points for each of the previously measured isotherms were repeated. In particular, thermodynamic states with low signal-to-noise ratios and also some thermodynamic states at high pressure.

The ultrasonic pulses which propagate into the samples showed that the signal-to-noise ratio worsens for decreasing pressures and increasing temperatures. When measurements

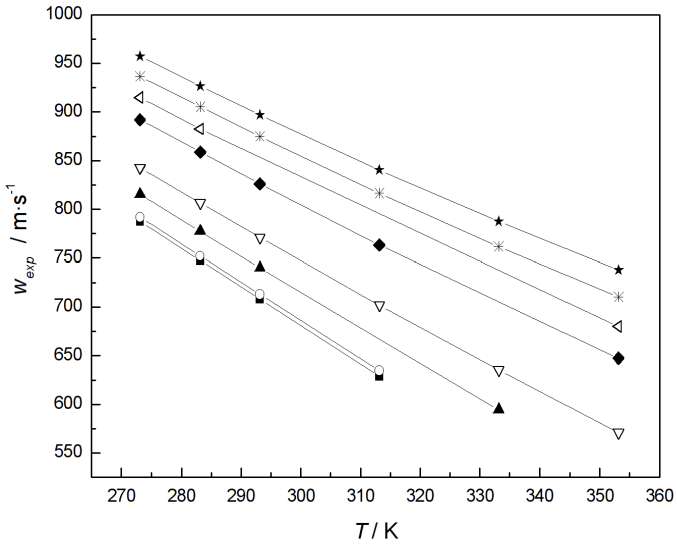

Figure 2: Speed of sound measurements as a function of temperature at constant pressure, namely: (■) 0.3 MPa, (○) 1 MPa, (▲) 5 MPa, (▽) 10 MPa, (⧫) 20 MPa, (◁) 25 MPa, (∗) 30 MPa, (⋆) 35 MPa.

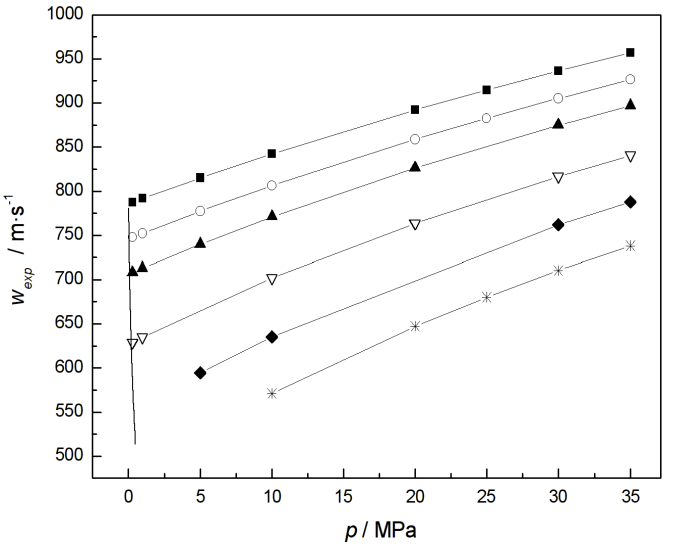

Figure 3: Speed of sound measurements as a function of pressure at constant temperature, namely: (■) 273.15 K, (○) 283.15 K, (▲) 293.15 K, (▽) 313.15 K, (⧫) 333.15 K, (∗) 353.15 K, (—) Saturation line.

became unreliable with unacceptably low signal-to-noise ratios, they were rejected.

As previously mentioned the working fluid exhibited polymerization at the high pressure conditions (over 25 MPa). Figure 4 shows polymer residues deposited on the surface of the cell reflector and on the pressure vessel stopper. Moreover, the polymerization also covered one side of the PZT transducer reducing again the signal-to-noise ratio. Since for the isotherm of 353 K, the signal-to-noise ratio of the first measurement cell was prohibitive, the measurements were repeated using a different cell with a different geometry.

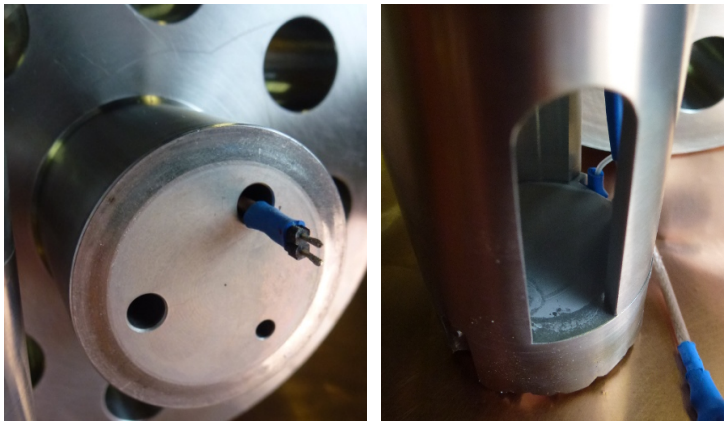

(a) (b)

Figure 4: R1233zd(E) polymers deposited on the pressure vessel top stopper (a) and on the reflector of the measurement cell (b).

To obtain a complete and reliable estimation of the experimental uncertainties, several thermodynamic state points were repeated using both ultrasonic cells. The repeatability for each cell was found to be within 0.002 % and the agreement using the two different cells was better than 0.06 %, that is, within the overall expanded uncertainty (0.08 %). For this reason, only one of the two obtained values is reported in Table 1.

As mentioned above, these measurements were compared with the predictions of the recent dedicated Fundamental Helmholtz Energy equation of state.[1] As reported in Figure 5, the results show deviations from the equation of state below 0.4 % for all temperatures, although the agreement is better at lower pressures than at higher pressures. These deviations are acceptable, particularly considering that the equation of state was developed without access to subcooled liquid speed of sound data.

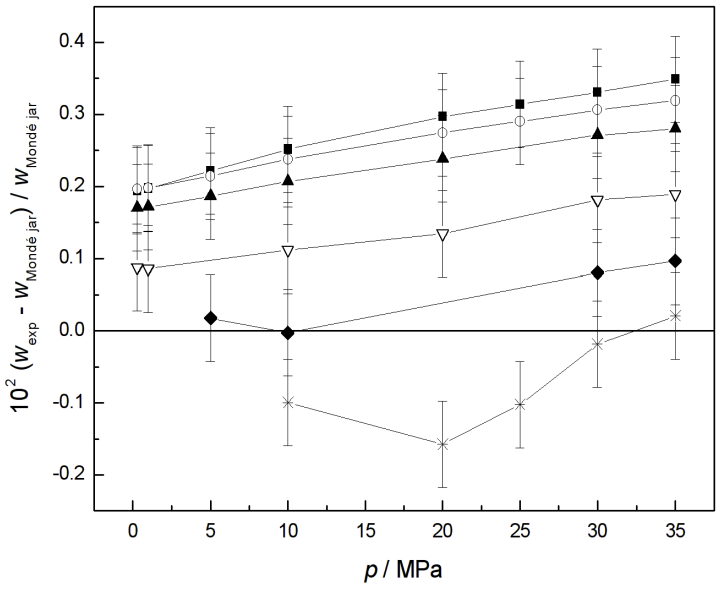

Figure 5: Comparison of the speed of sound measurements obtained in this work with respect to the values predicted by the dedicated Fundamental Helmholtz Energy equation of state.[1] (■) 273.15 K, (○) 283.15 K, (▲) 293.15 K, (▽) 313.15 K, (⧫) 333.15 K, (∗) 353.15 K.

Applied corrections and uncertainty budget

Experimental measurements of times-of-flight and traveled path-lengths can be used, for determining the speed of sound, only after applying them the corrections. In this view, the expression that better represents the speed of sound measurements can be resumed with the following model:

$$w_{\text{exp}} = \frac{2\Delta L}{\tau + \delta\tau} = w_{\text{exp}}(\Delta L, \tau, p, T) \tag{2}$$

where w_{exp} represents the experimental speed of sound, $\Delta L = (L_2 - L_1)$ represents the acoustic path length difference and τ represents the time-of-flight, determined independently. The correction term $\delta\tau$ comes from the wave-like nature of the spreading signal and it is due to diffraction effects of the ultrasonic tone burst showing a phase advance φ of the ultrasonic pulses, relative to a plane wave traversing the same distance.

The diffraction correction $\delta\tau$ can be calculated using the following equations[10]

$$\delta\tau = \frac{\varphi\left(2L_2\right) - \varphi\left(2L_1\right)}{\omega_0} \tag{3}$$

$$\varphi\left(L\right) = \mathrm{Arg}\left(1 - \frac{4}{\pi}\int_0^{\pi/2} \exp\left[-i\left(\frac{2\omega_0 b^2}{wL}\right)\cos^2\left(\theta\right)\right]\sin^2\left(\theta\right)\mathrm{d}\theta\right), \tag{4}$$

where ω_0 is the angular frequency of the carrier beam, L_1 and L_2 are the distances that separate the source from each reflector, and b is the radius of the source.

A closed form for the integral appearing in eq. (4) can be obtained by means of a Computer Algebra System (CAS) as

$$\varphi\left(L\right) = \mathrm{Arg}\left(1 - e^{iA/(2L)}J_0(A/(2L)) - ie^{iA/(2L)}J_1(A/(2L))\right) \tag{5}$$

where $A = (2\omega_0 b^2)/w$, while J_0, and J_1, are Bessel functions of 0- and 1-order, respectively.

Although it is possible to determine the exact value for the integral (4), this does not mean that fly-time $\delta\tau$ corrections can completely take into account diffraction effects. An important recommendation can be found in,[10] where it is stated that the experiment should be designed so that the corrections, due to diffraction effects, is negligible with respect to other sources of uncertainty. In fact, equation (4) is simply an approximation of a very complex phenomenon that cannot be described by simple models, if it is considered in all its aspects.

Equation (5) accounts just for the phase-shift induced on the points of the z-axis, while it would be more exact to consider that the transducer has extensions out of its main axis and that the transduced electric signal is an integral over its wall surface. Moreover, equation (5) is obtained considering that the diameter of the transducer is small with respect to that one of the cell but sometimes, for high pressure measurements, it is necessary to reduce the dimension of the cells and this hypothesis, under certain conditions, may not hold time may not be respected. Anyway, for the measurement cells used herein, the diffraction correction accounted for less than 0.0085 % of the measured

transit time difference.

Finally, p and T are state variables serving two functions: as thermodynamic parameters for speed of sound and also as perturbing quantities for ΔL.

As a matter of fact, considering the difference of the source-reflector distances (ΔL), it depends on the temperature and pressure conditions through the linear thermal dilatation coefficient α and the linear compressibility coefficient β of the material, which the ultrasonic cell is made of, according the following relation:

$$\Delta L(p,T) = \Delta L(p_0,T_0)(1 + \alpha\Delta T - \beta\Delta p) \tag{6}$$

where

$$\alpha = \frac{1}{3V}\left(\frac{\partial V}{\partial T}\right)_p, \tag{7}$$

$$\beta = \frac{1}{3V}\left(\frac{\partial V}{\partial p}\right)_T, \tag{8}$$

with p_0 and T_0 representing reference pressure and temperature values, respectively, at which the geometrical dimensions of the cell have been obtained by the calibration procedure. The path lengths have been calibrated with ultra-quality degassed Millipore water using the data of IAPWS formulation,[13] according to the procedure described in[14] and[15] over the full investigated temperature range and for pressures of 0.1 MPa, 20 MPa, and 60 MPa. Direct, independent measurement at ambient conditions of the spacers were made demonstrating consistency with the water calibration. Equation (6) must be included as a correction in equation (2), resulting in the following model of the indirect measurement of the speed of sound:

$$w_{\text{exp}} = w_{\text{exp}}(\Delta L_0, \tau, p, T, \alpha, \beta), \tag{9}$$

where α and β have to be considered as influence quantities.[16]

When time-of-flight, temperature and pressure corrections are applied, it is possible

to proceed to the estimation of the uncertainty associated to the measurement. Applying the procedure for the propagation of uncertainty[17] to the equation (9), we obtain

$$\left(\frac{u\left(w_{\mathrm{exp}}\right)}{w_{\mathrm{exp}}}\right)^2 = \left(\frac{u\left(\Delta L_0\right)}{\Delta L}\right)^2 + \left(\frac{u\left(\tau\right)}{\tau}\right)^2 + \left(\frac{T}{w_{\mathrm{exp}}}\frac{\partial w_{\mathrm{exp}}}{\partial T}\right)^2 \left(\frac{u\left(T\right)}{T}\right)^2 + \left(\frac{p}{w_{\mathrm{exp}}}\frac{\partial w_{\mathrm{exp}}}{\partial p}\right)^2 \left(\frac{u\left(p\right)}{p}\right)^2 . \tag{10}$$

Table 3 lists the major contributions to the combined expanded uncertainty.

Table 3: **Uncertainty budget.**

Uncertainty source ($k = 2$)	Relative magnitude
Determination of the acoustic path length	0.043 %
Determination of the temporal delay	0.003 %
Temperature measurement	0.031 %
Pressure measurement	0.040 %
Repeatability	0.002 %
Reproducibility	0.060 %
Estimated Relative Overall Uncertainty	0.08 %

Pressure measurements have uncertainties of 0.0004 MPa at ambient condition and of 0.025 MPa for the highest pressure conditions. Temperature measurements are assumed to have an uncertainty of 0.04 K, corresponding to the calibration accuracy. The PT100s were calibrated by comparison with a 25 Ω standard platinum resistance thermometer (SPRT). The uncertainty in the temperature of the fluid sample also included the effect of temperature gradients, that it is ranging between 10 mK and 60 mK, depending on the isotherms. The estimated relative uncertainty, which can be considered as representative over the entire pressure range, was calculated by a weighted mean; the sensibility factor $\left(\frac{T}{w_{\mathrm{exp}}}\frac{\partial w_{\mathrm{exp}}}{\partial T}\right)$ and $\left(\frac{p}{w_{\mathrm{exp}}}\frac{\partial w_{\mathrm{exp}}}{\partial p}\right)$ which appears in Eq. (10) was calculated from the experimental speed of sound values by means of polynomial interpolations. Each component of the uncertainty budget was multiplied by a coverage factor chosen to better fit the experimental conditions. Specifically, uncertainties associated with acoustic path length, temperature and pressure were evaluated with a coverage factor $k = 2$ (for a 95 % confidence interval), while time-delay uncertainty has $k = 4$ to include effects of a low signal-to-noise ratio. Combining all the contributions, the relative uncertainty of the speed of sound is estimated to be better than 0.08 % over the entire examined $p - T$

region, accounting for the small differences observed using independent speed of sound sensors.

To the best of the authors' knowledge, there are no other experimental measurements available in the scientific literature for compressed liquid speed of sound of R1233zd(E).[1] developed a 15-term equation of state explicit in the Helmholtz energy with the density and temperature as independent variables for R1233zd(E). Their equation is based on their experimental results of densities, measured over the temperature range of (215 and 444) K, with pressures from (0.3 to 24.1) MPa; sound speed measured in the vapor phase at temperatures between (290 and 420) K and pressures from (0.07 to 2.1) MPa; vapor pressures in the temperature range from (280 to 438) K. Even if Mondéjar's equation was not developed using compressed liquid speed of sound data, it can be used to estimate these values. Figure 4 shows the deviations of the experimental values from Mondéjar's equation. The largest deviations correspond to the larger pressure values, as expected; however, it should be noted that these deviations can be considered to be acceptable, particularly since the equation of state was developed without access to compressed liquid speed of sound data. Thus, the authors recommend that Mondéjar's equation of state be updated using the experimental compressed liquid speed of sound data reported herein.

Conclusion

This paper reports compressed liquid speed of sound measurements for the low-pressure, low global warming potential working fluid R1233zd(E) using a double-reflector pulse-echo overlap technique. Trans-1-chloro-3,3,3-trifluoropropene has been approved by the U.S. Environmental Protection Agency[18] as a new blowing agent in foam insulation and as a refrigerant in chillers,[9] because of its relatively short atmospheric lifetime and its low global warning potential. The measurements were obtained by using two sensors with different path lengths and the results have been compared with the most recent dedicated equation of state[1] despite the fact that it was developed without access to subcooled liquid speed of sound measurements. Namely, it is based on speed of sound measurements

taken in the gas phase along eight isotherms from (290 to 420) K for pressures from (0.07 to 2.07) MPa, with a relative combined expanded uncertainty of 0.026 %. Mondéjar's equation of state represents their vapor phase speed of sound experimental data with a relative root-mean-square deviation of 0.131 %. The authors are confident that these results will be useful for developing a more refined and accurate formulation of a dedicated equation of state.

Acknowledgement

The authors thank Central Glass Co., Ltd. for providing the sample.

Literature Cited

(1) Mondéjar, M.E.; McLinden, M.O.; Lemmon, E.W., Thermodynamic Properties of *trans*-1-Chloro-3,3,3-trifluoropropene (R1233zd(E)): Vapor Pressure, (p, ρ, T) Behavior, and Speed of Sound Measurements, and Equation of State. *J. Chem. Eng. Data*, **2015**, *60*, 2477-2489.

(2) ANSI/ASHRAE Addenda a, b, c, d, e, f, g, h, i, j, k, l, m, n to Standard 34-2013 Designation and Safety Classification of Refrigerants. ASHRAE, Atlanta, GA, **2015**.

(3) Orkin, V.L.; Martynova, L.E.; Kurylo, M.J., Photochemical properties of trans-1-chloro-3,3,3-trifluoropropene (trans-CHCl=CHCF3): OH reaction rate constant, UV and IR absorption spectra, global warming potential, and ozone depletion potential. *J. Phys. Chem. A*, **2014**, *118*, 5263-5271.

(4) Di Nicola, G.; Fedele, L.; Brown, J.S.; Bobbo, S.; Coccia, G.; Saturated pressure measurements of trans-1-chloro-3,3,3-trifluoroprop-1-ene (R1233zd(E)). *J. Chem. Eng. Data*, **2017**, *62*, 2496-2500.

(5) Hulse, R.J.; Basu, R.S.; Singh, R.R.; Thomas, R.H.P., Physical properties of HCFO-1233zd(E). *J. Chem. Eng. Data*, **2012**, *57*, 3581-3586.

(6) Romeo, R.; Giuliano Albo, P.A.; Lago, S.; Brown, J.S., Experimental liquid densities of cis-1,3,3,3-tetrauoroprop-1-ene (R1234ze(Z)) and trans-1-chloro-3,3,3-trifluoropropene (R1233zd(E)). *Int. J. Refrig.*, **2017**, *76*, 176-182.

(7) Tanaka, K.; $p\rho T$ property of trans-1-chloro-3,3,3-trifluoropropene (R 1233zd(E)) near critical density. *J. Chem. Eng. Data*, **2016** *61*, 3570-3572.

(8) Kondou, C.; Nagata, R.; Nii, N.; Koyama, S.; Higashi, Y., Surface tension of low GWP refrigerants R1243zf, R1234ze(Z), and R1233zd(E). *Int. J. Refrig.*, **2015**, *53*, 80-89.

(9) Lemmon, E.W.; Huber, M.L.; McLinden, M.O., NIST Standard Reference Database 23, Reference Fluid Thermodynamic and Transport Properties (REFPROP), version 9.1; National Institute of Standards and Technology: Gaithersburg, MD, 2010 (R1233zd(E) fluid file updated November 9, 2015).

(10) Trusler, J.P.M., 1991. Physical Acoustics and Metrology of Fluids, Adam Hilger, Bristol.

(11) Kinsler, L.E.; Frey, A.R.; Coppens, A.B.; Sanders, J.V., 1982. Fundamentals of Acoustics (third editions). John Wiley & Sons, New York.

(12) Giuliano Albo, P.A.; Lago, S.; Romeo, R.; Lorefice, S., High pressure density and speed-of-sound measurements in n-undecane and evidence of the effects of near-field diffraction, *J. Chem. Thermodynamics*, **2013**, *58*, 95-100.

(13) Wagner,W.; Pruss, A., The IAPWS formulation 1995 for the thermodynamic properties of ordinary water substance for general and scientific use. *J. Phys. Chem. Ref. Data*, **2002**, *31*, 387-535.

(14) Lago, S.; Giuliano Albo, P.A.; Madonna Ripa, D., Speed-of-Sound Measurements in n-Nonane at Temperatures between 293.15 and 393.15 K and at Pressures up to 100 MPa, *Int. J. Therm.*, **2006**, *27*, 1083-1094.

(15) Lago, S.; Giuliano Albo, P.A., Thermodynamic properties of acetone calculated from accurate experimental speed of sound measurements at low temperatures and high pressures. *J. Chem. Thermodynamics*, **2009**, *41*, 506-512.

(16) Benedetto, G.; Gavioso, R.M.; Giuliano Albo, P.A.; Lago, S.; Madonna Ripa, D.; Spagnolo, R., Speed of sound in pure water at temperatures between 274 and 394 K and pressures up to 90 MPa. *Int. J. Therm.*, **2005**, *26*, 1667-1680.

(17) BIPM, IEC, IFCC, ILAC, ISO, IUPAC, IUPAP and OIML 2008 Evaluation of Measurement Data - Guide to the Expression of Uncertainty in Measurement (Geneva: International Organization for Standardization) (Joint Committee for Guides in Metrology, JCGM 100:2008).

(18) U.S. Environmental Protection Agency Acceptable Substitutes for CFC-114 and CFC-11 in Chillers and Other Refrigerants. http://www.epa.gov/ozone/snap/refrigerants/lists/114cent.html (accessed October 29, 2014).